The Effect of CT Dose Reduction on Proton Therapy Dose Calculation

Masoud Elhamiasl, Sara Teruel Rivas, Koen Salvo, Edmond Sterpin, and Johan Nuyts

***Abstract*—In adaptive proton therapy, a CT scan is acquired in each treatment session to enable detection of and correction for changes in the anatomy which would otherwise cause significant changes to the dose distribution. This CT is not used to delineate lesions or tissues at risk, it is only used to compute proton stopping powers for dose calculations. Because a treatment typically involves 30 to 40 treatment sessions, the total dose associated with these CT-scans is significant, in particular, if 4D CT is used to account for breathing effects. We hypothesized that the signal-to-noise ratio provided by conventional CT protocols is higher than needed for this application. To verify this hypothesis and enable a patient dependent reduction of the CT dose, a CT dose reduction simulation tool is developed to simulate lower-dose CT scans from an existing standard-dose scan. The simulated lower-dose scans are then used for treatment planning and the results are compared with that of the standard dose scan. The preliminary results show that the dose reduction by a factor up to 10 does not have a significant effect on proton dose distribution.**

***Index Terms*—CT, dose reduction, low-dose simulation, proton therapy, treatment planing.**

I. Introduction

PROTON therapy is an advanced form of radiotherapy which utilizes proton beams to destroy cancer cells. In contrast to photons, protons can deliver their maximum dose to the tumor cells which results in a significant dose reduction to healthy tissue [1]. However, systematic and random errors on the stopping powers can have a significant effect on the estimated dose distribution [2]. For example, a small motion of the tumor inside the patient's body can have a significant effect on the dose distribution, because the stopping power of the tissues traversed by the protons can vary substantially, and even relatively small changes of the trajectory of the protons through the body can have an important effect on the position of the Bragg peak. Consequently, it is important to do adaptive planning to make sure that the treatment is based on an accurate estimate of the tissue compositions and densities.

Proton therapy treatment planning is typically based on stopping power estimation from CT images. To minimize range uncertainties due to anatomical variations, daily CT acquisition would be paramount. Unfortunately, the series of CT scans result in a substantial accumulated patient dose, especially for lung tumors where a 4D CT-scan is required. Low-dose CT is desirable, however, lowering the dose results in a lower signal-to-noise ratio (SNR) and therefore in a reduced image quality. Because these CT scans are not used for tumors delineation, we believe that their required signal-to-noise ratio is lower than that needed for typical radiological images, and therefore there is room for dose reduction. In this research, we aim to determine the lowest exposure scan which still produces sufficient information for proton therapy dose calculations. As argued in [2], the estimated proton stopping powers are a non-linear function of the reconstructed Hounsfield units. Therefore, it is not only important the reconstructed images have a low bias, but also their noise magnitude should be sufficiently small to avoid noise-induced bias in the derived stopping powers. Accordingly, a lower-dose CT simulation tool has been developed and validated to simulate lower-dose scans from an existing standard dose scan. The interested reader is referred to [3] for further details on the proposed model. The simulated lower-dose scan will then be used for treatment planning and the results will be compared with that of the standard-dose scan.

M. Elhamiasl and J. Nuyts are with the Department of Imaging and Pathology, Nuclear Medicine & Molecular imaging, Medical Imaging Research Center (MIRC), KU Leuven, Leuven 3000, Belgium.

S. Teruel Rivas is with the Institut de Recherche Experimentale et Clinique (IREC), Center of Molecular Imaging, Radiotherapy and Oncology (MIRO), Universite catholique de Louvain, Brussels 1200, Belgium.

K. Salvo is with the Department of Radiotherapy, UZ Leuven, Leuven 3000, Belgium.

E. Sterpin is with the Department of Oncology, Laboratory of Experimental Radiotherapy, KU Leuven, Leuven 3000, Belgium.

II. Low-dose CT Simulation

A. Low-dose Simulation Algorithm

Reducing the X-ray tube load is the most effective way of radiation reduction dose to the patients. Tube load reduction can be modeled by estimating the (noise equivalent) number of photons in the high exposure scan and then applying a thinning technique to it (i.e. to randomly eliminate photons using a well-chosen survival probability). Therefore, the log-converted CT raw data should first be converted into the form of transmission data. Assuming a monochromatic beam, the mean number of detected photons in the high dose scan can be written as

$$I^{(\beta)} = I_0^{(\beta)} \exp(-\rho) \tag{1}$$

where the superscript (β) identifies the tube load level in mAs. I_0 and ρ represent incident X-ray intensity and log-converted raw data, respectively. We assume that I_0 depends linearly on the tube load, i.e. $I_0^{(\beta)} = \beta I_0^{(1)}$. Accordingly, estimation of the number of photons from the log-converted data requires a noise-free estimate of $I_0^{(1)}$, the incident X-ray intensity for a unit tube load. The variance of an air scan without any attenuating object can be used to estimate $I_0^{(1)}$. Assuming the CT transmission data as a combination of a Poisson and a

normal distribution, the variance of the transmission data in an air scan is given by

$$\mathrm{var}[\exp(-\rho_{air}^{(\alpha)})] = \mathrm{var}[\frac{I_{air}^{(\alpha)}}{I_0^{(\alpha)}}] = \frac{\alpha I_0^{(1)} + \sigma_e^2}{(\alpha I_0^{(1)})^2} \qquad (2)$$

where α and σ_e^2 represent the tube load and the variance of electronic noise, respectively. $I_0^{(1)}$ and σ_e^2 can be estimated by performing some air scans at different levels of tube load. Therefore, the number of photons in the transmission scan with tube load β mAs can be estimated using (1). Thinning with survival probability α/β can then be applied to produce a (more) noisy low-dose scan of α mAs. Thinning means the random elimination of some of the detected photons where the chance of not being eliminated is the same for each photon. A binomial random generator was used to compute the effect of the thinning. This approach accounts for the fact that the higher exposure scan is already noisy. Electronic noise is modeled as a shifted Poisson distribution and the thinning is then applied to all photons. The thinning also reduces the contribution of the electronic noise, which can be restored by adding a noisy number of additional photons. After that, the final Poisson distribution is shifted back. This yields the following equation:

$$I_{sim}^{(\alpha)} = \mathcal{B}\Big(\beta I_0^{(1)} \exp(-\rho) + \sigma_e^2, \frac{\alpha}{\beta}\Big) + \mathcal{P}\{(1-\frac{\alpha}{\beta})\sigma_e^2\} - \sigma_e^2 \quad (3)$$

The first term reduces the number of photons observed in the converted raw transmission data. The second term adds a noisy number of photons to compensate for the thinning of the electronic noise and the last term subtracts the mean number of electronic noise photons, to ensure that the electronic noise has zero mean.

The relation between beam intensity and the effective number of photons has been derived using blank scans. However, in patient scans, the photon beams reaching the detector are harder than in blank scans, because of the beam hardening effect. A harder beam contains fewer photons for the same intensity and is therefore subject to a higher amount of quantum noise [4]. Knowing the attenuation value and also the bowtie thickness in each beam path and assuming that all patient attenuation is due to water [5], the (noise equivalent) number of photons can be adjusted to account for the beam hardening effect.

In the above, the noise contribution of any detector element was assumed to be independent of that of the other detectors. However, the noise of neighboring CT detector pixels is correlated due to crosstalk between detector pixels [4]. Since the noise added by thinning is uncorrelated, it reduces the noise correlations. It is important to restore this noise correlation in the lower-dose simulated scan because the noise propagation through the image reconstruction is not the same for correlated and uncorrelated noise. To obtain the appropriate correlation in the simulated scan, we convolve the thinning noise with a smoothing mask w, which is designed to impose the desired covariance without changing the variance. It can be proved that w should satisfy $[w \otimes w]_{i-j} = r_{ij}$, where r_{ij} represents the correlation matrix between neighboring pixels.

The CT scanners are usually equipped with a preprocessing software to avoid negative values to be passed to the log when the detected signal is too small [6]. In agreement with this, we observed that the correlation between neighboring pixels increases when the number of photons is below a particular threshold. The number of photons for which the filter must be activated can be determined by analyzing the correlation between neighboring pixels. To obtain a similar result as that produced by the unknown vendor software, we introduced a simple intensity-dependent filter: the detected signal is smoothed by a simple 3×3 top-hat filter and a weighted sum of the original and smoothed views is computed. The intensity-dependent weight is designed to prevent the variance to increase beyond a predefined threshold. In [3] the method is described in more detail.

B. Validation of the Low-dose Simulation

The lower-dose CT simulation model was validated by performing phantom studies. In each experiment, a standard-dose scan along with corresponding lower-dose scans were performed. The standard-dose scan was used as an input to simulate the lower-dose scans. The simulated scans were then reconstructed and compared with corresponding real lower-dose acquired scans.

Two phantom studies were conducted to evaluate the accuracy of the lower-dose simulation tool. The tube voltage was set at 120 kVp in all experiments. In the first experiment, a realistic head phantom (Proton Therapy Dosimetry Head, Model 731-HN) was scanned on Siemens SOMATOM Force scanner with a routine clinical protocol [helical, tube current modulation, Pitch: 0.55]. The high-dose scan of 192 effective mAs was used as the input standard-dose scan to simulate the lower-dose scans. The simulated scans were then reconstructed using Siemens reconstruction software and compared with corresponding real lower-dose images. In the second experiment, the low-dose CT simulation tool was validated on Siemens SOMATOM DRIVE scanner. A water-filled PMMA cylinder with a diameter of 21 cm was scanned using a sequential CT head-neck protocol. The lower-dose scans were simulated from a high-dose scan of 300 mAs and reconstructed using in-house FDK reconstruction.

The standard deviations of the reconstructed image in uniform ROIs and were used for the comparison. Table I compares the noise level for the acquired and the simulated images. The standard deviation of the reconstructed images in uniform ROIs revealed a close agreement of the noise level in the observed and simulated lower-dose scans where the relative error was on the order of $\sim$1% for sequential and $\sim$3% for helical scans. Fig. 1 shows the high-dose scan of 192 mAs and its corresponding measured and simulated lower-dose scans. It can be seen that the noise level in the reconstructed images has been increased by reducing the tube load. In [3], [7], [8] additional validation experiments are presented.

III. Effect of CT Dose Reduction on Dose Calculations

The high-dose and simulated lower-dose scans of the realistic head phantom were used to investigate the effect of CT dose

TABLE I

THE DETAILED COMPARISON OF NOISE LEVELS OF THE ACQUIRED AND THE SIMULATED LOW-DOSE IMAGES AT DIFFERENT LEVELS OF TUBE LOAD FOR HEAD AND 21 CM WATER PHANTOMS. THE STANDARD DEVIATION OF THE NOISE IN UNIFORM ROIS WERE USED FOR COMPARISON.

head phantom				21 cm water phantom						
	region 1				center			periphery		
Tube load	real	sim	error	Tube load	real	sim	error	real	sim	error
192	3.38	-	-	300	25.46	-	-	22.19	-	-
117	4.25	4.23	0.2%	250	28.17	27.82	0.8%	25.02	24.91	0.4%
93	4.80	4.68	2.5%	200	31.03	30.96	0.2%	27.88	27.79	0.3%
70	5.48	5.41	1.2%	150	36.07	35.79	0.7%	32.24	32.25	0.0%
47	6.76	6.56	2.9%	100	44.12	44.12	0.0%	39.55	39.70	0.4%
24	9.48	9.18	3.1%	50	62.83	63.66	1.3%	55.94	57.25	2.3%
20	10.44	9.95	4.6%	20	85.16	83.88	1.5%	81.78	80.84	1.1%

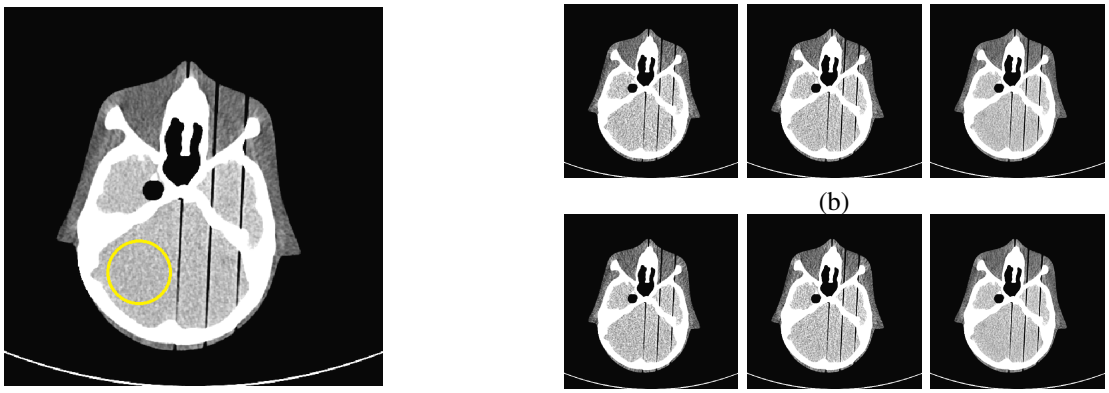

(a) (b) (c)

Fig. 1. Presentation of (a) the measured high-dose image of 192 effective mAs and (b) corresponding acquired and (c) simulated lower-dose images of 20, 24, and 47, effective mAs (from left to right) using the proposed framework (window level: 30 HU, window width: 100 HU). The yellow circle represents the uniform ROI.

reduction on proton therapy dose calculations. The standard-dose scan of 192 mAs was used for dose calculation and considered as the ground truth. A small region was defined as the tumor and a treatment plan was generated. The prescription dose was 70 Gy to Planning Target Volume (PTV) and reoptimized on every CT with Monte Carlo simulation, using a 3 mm dose grid resolution, 2 beams 90° (left) and 270° (right) beam. The simulations were performed on RayStation 8B(R) SP1, using the beam model of the clinical beam line of UMCG (University Medical Center Groningen). Subsequently, dose distributions were recalculated for the simulated lower-dose images and compared with the ground truth.

The Dose Volume Histogram (DVH) metrics for the standard-dose scan and the simulated scans are reported in Table II. Fig. 2(a) represents the DVH curve for the high-dose scan of 192 mAs and the real and the simulated scans of 20 mAs. It can be seen that the dose reduction by a factor up to 10 has a negligible effect on the dose calculation where the DVH curve of the standard-dose and the lower-dose scans are on top of each other. The difference between the DVH curves of the high-dose scan and the simulated lower-dose scans, for the same volume%, have been presented in Fig. 2(b). Comparing the high-dose scan of 192 mAs with the lower-dose scan of 20 mAs shows that the maximum difference between the DVH curves is about 0.836 Gy which only happens in 2% of CTV volume. Fig. 3 represents the dose distribution maps for the high-dose scan of 192 mAs and the real and the simulated scans of 20 mAs.

IV. CONCLUSION

In this paper, we investigated the effect of CT dose reduction on proton therapy treatment planning. A lower-dose CT simulation tool was used to simulate low-dose CT scans from a standard-dose scan. The bowtie filter, the electrical noise, the correlated noise, the beam hardening effect, and the signal-dependent filter were included in the proposed model. The simulated lower-dose scans were used for proton therapy treatment planning. Our preliminary results show that the CT dose reduction does not have a significant effect on the estimated dose distributions. A more systematic and quantitative analysis of the effect of dose reduction on proton therapy treatment planning for more complex inhomogeneous anatomical structures is ongoing.

ACKNOWLEDGMENT

This project is supported by Fonds Baillet-Latour. The authors would like to warmly thank Xavier Geets for the initial design of the research, Walter Coudyzer for his contribution in data collection and Karl Stierstorfer and Frederic Noo for their valuable comments and suggestions.

TABLE II
THE DETAILED COMPARISON OF DVH METRICS FOR THE ACQUIRED STANDARD-DOSE AND THE SIMULATED LOWER DOSE SCANS.

Tube load	PTV D99	PTV D98	PTV D95	Average	PTV D50	PTV D2	PTV D1
192 (REF)	70.95	71.41	71.62	73.31	73.37	75.04	75.37
140 (sim)	70.91	71.22	71.44	73.24	73.24	75.61	76.36
117 (sim)	71.05	71.41	71.68	73.53	73.54	75.72	76.05
93 (sim)	71.10	71.64	71.77	73.37	73.32	75.40	75.72
70 (sim)	70.99	71.26	71.67	73.30	73.38	74.85	75.21
47 (sim)	70.80	70.95	71.27	73.51	73.69	75.51	75.72
24 (sim)	71.36	71.71	71.95	73.53	73.41	75.73	75.97
20 (sim)	70.72	71.06	71.41	73.24	73.14	75.88	75.90
20 (real)	71.19	71.33	71.70	73.26	73.25	75.49	75.67

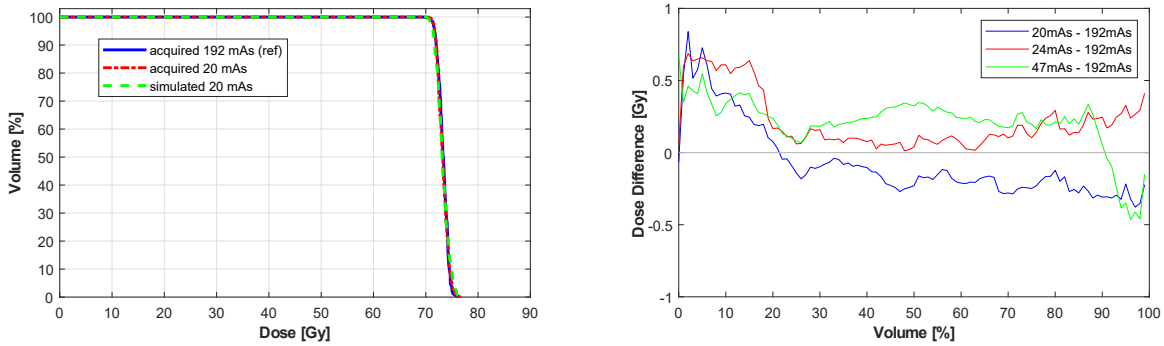

(a) (b)

Fig. 2. An illustration of the effect of CT dose reduction on the DVH curves. (a) Presentation of the DVH curves for the high-dose scan of 192 mAs, the acquired low-dose scan of 20 mAs, and the simulated scan of 20 mAs. (b) Demonstration of the difference between the DVH curve of the high dose scan and the simulated lower-dose scans.

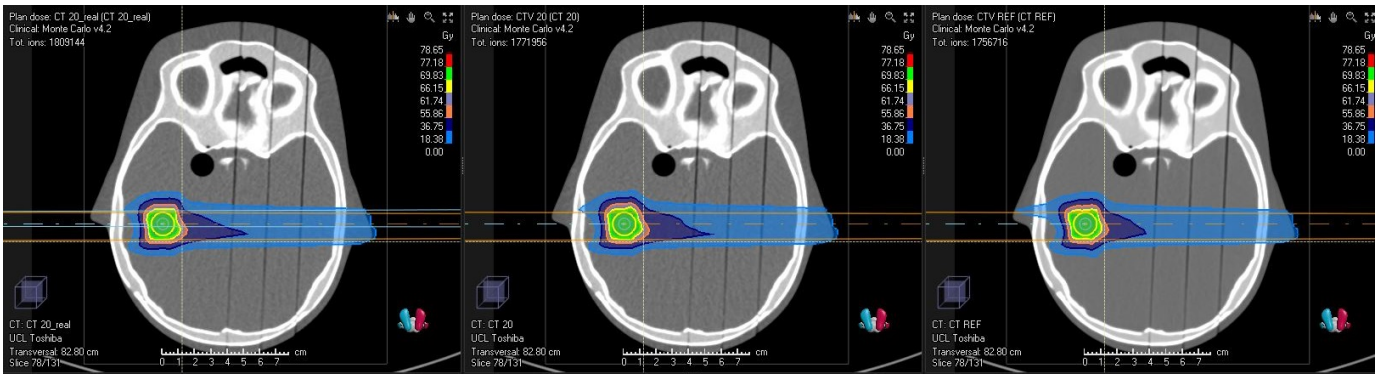

(a) (b) (c)

Fig. 3. Dose distribution maps corresponding to (a) acquired low-dose scan of 20 mAs, (b) simulated low-dose scan of 20 mAs, and (c) acquired standard-dose scan of 192 mAs (ground truth).

REFERENCES

[1] H. Paganetti, *Proton Beam Therapy*, ser. 2399-2891. IOP Publishing, 2017. [Online]. Available: http://dx.doi.org/10.1088/978-0-7503-1370-4

[2] S. Brousmiche, K. Souris, J. O. de Xivry, J. A. Lee, B. Macq, and J. Seco, "Combined influence of ct random noise and hu-rsp calibration curve nonlinearities on proton range systematic errors," *Physics in Medicine & Biology*, vol. 62, no. 21, p. 8226, 2017.

[3] M. Elhamiasl and J. Nuyts, "Low-dose x-ray CT simulation from an available higher-dose scan," *Physics in Medicine & Biology*, 2020. [Online]. Available: http://iopscience.iop.org/10.1088/1361-6560/ab8953

[4] B. R. Whiting, P. Massoumzadeh, O. A. Earl, J. A. O'Sullivan, D. L. Snyder, and J. F. Williamson, "Properties of preprocessed sinogram data in x-ray computed tomography," *Medical physics*, vol. 33, no. 9, pp. 3290–3303, 2006.

[5] T. M. Benson and B. K. De Man, "Synthetic ct noise emulation in the raw data domain," in *IEEE Nuclear Science Symposuim & Medical Imaging Conference*. IEEE, 2010, pp. 3169–3171.

[6] L. Yu, M. Shiung, D. Jondal, and C. H. McCollough, "Development and validation of a practical lower-dose-simulation tool for optimizing computed tomography scan protocols," *Journal of computer assisted tomography*, vol. 36, no. 4, pp. 477–487, 2012.

[7] M. Elhamiasl, K. Salvo, W. Coudyzer, and J. Nuyts, "Low-dose CT simulation from an available higher dose CT scan," in *2019 IEEE Nuclear Science Symposium and Medical Imaging Conference (NSS/MIC)*, 2019, pp. 1–3, ISSN: 2577-0829.

[8] M. Elhamiasl and J. Nuyts, "Simulating lower-dose scans from an available CT scan," in *15th International Meeting on Fully Three-Dimensional Image Reconstruction in Radiology and Nuclear Medicine*, vol. 11072. International Society for Optics and Photonics, 2019, p. 110720X.